Dynamics of detachment in TCV with N_2 seeding and flux expansion

O. Février[1], C. Theiler[1], C. K. Tsui[2,1],K. Verhaegh[3,1], J.A. Boedo[2], B. Duval[1], J. Harrison[4], B. Labit[1], B. Lipschultz[3], R. Maurizio[1], H. Reimerdes[1], the TCV Team* and the EUROfusion MST1 Team†

[1]*EPFL, Swiss Plasma Center (SPC), CH-1015 Lausanne, Switzerland.*

[2]*University of California-San Diego, La Jolla, California 92093, USA.*

[3]*York Plasma Institute, University of York, Heslington, York, YO10 5DQ, UK.*

[4]*CCFE, Culham Science Centre, Abingdon, OX14 3DB, Oxon UK.*

As the operation of future devices will require target heat fluxes of less than 10-20 MW/m^2, finding ways of dissipating the power before it reaches the divertor targets is a critical issue. This can be achieved by injecting low-Z impurities in the divertor to radiate part of the power. Impurity seeding can also facilitate the access to a detached regime where a reduction of target heat loads and a drop of the target ion flux is associated with the development of momentum losses along the SOL. Such a regime is expected to be necessary in ITER or DEMO, and in both experiments, it is expected that impurity seeding will be required to access it.

Experimental setup We explore N_2-seeding detachment in L-Mode, Lower Single-Null, Ohmic-heated discharges, with a plasma current $I_P \approx 340$ kA on TCV. The ∇B-drift is directed away from the X-Point. The overall plasma geometry is plotted in figure 1. The plasma is fuelled by injecting D_2 in the common flux region, the fueling rate being controlled by a feedback loop based on the line-averaged density $\langle n_e \rangle$. In the N_2-seeding discharges, N_2 is injected in the private flux region, following a prescribed, feed-forward ramp. Three different cases are studied: i) a $\langle n_e \rangle$-ramp, where $\langle n_e \rangle$ is linearly increased from $\approx 5 \times 10^{19}$ m^{-3} (Greenwald fraction $f_G = 30\%$) to $\approx 12 \times 10^{19}$ m^{-3} ($f_G = 70\%$), as shown on panel a) of figure 2; ii) A "high"-density N_2-seeding ramp, where the N_2 flux is linearly increased (up to saturation) (panel b)) over time while $\langle n_e \rangle$ is kept approximately constant ($\approx 9 \times 10^{19}$ m^{-3}, $f_G = 45\%$, panel a) of figure 2); iii) A "low"-density N_2-seeding ramp, where the N_2 flux is linearly increased over time while $\langle n_e \rangle$ is kept approximately

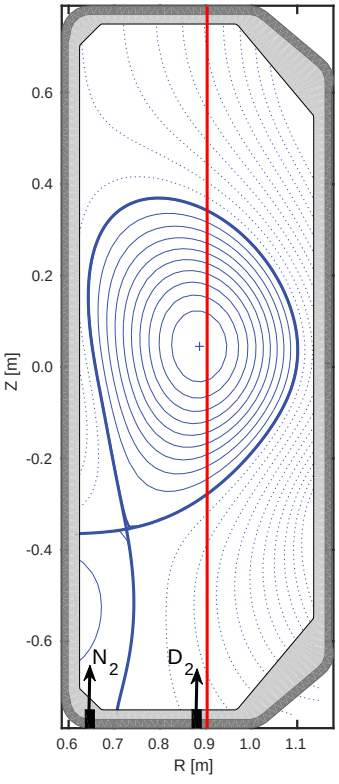

Figure 1: Plasma geometry. The two gas valves used to inject N_2 or D_2 are indicated. The red line indicates the interferometer line used to determine the line-averaged density.

*See the author list of S. Coda et al, 2017 *Nucl. Fusion* **57** 102011.
†See the author list of H. Meyer et al 2017 *Nucl. Fusion* **57** 102014.

constant ($\approx 4 \times 10^{19}$ m^{-3}, $f_G = 22\%$). In both seeding cases, the N_2 seeding starts at $t = 0.8$ s. Unless stated otherwise, the outer target flux expansion (f_x) is 10. This geometry is known to a significant drop of the outer target ion flux as $\langle n_e \rangle$ is increased [1, 2].

Main observations In panel f) of figure 2, we plot the evolution of the integrated ion flux to the outer target, Γ_t^o, as a function of time for the different cases. All three cases show a reduction of the target ion flux, either after a certain density threshold ($\langle n_e \rangle$ ramp) or a certain N_2 flux has been reached. In the high-density, N_2 seeded case, the ion flux decreases as soon as the seeding starts, while the low-density case starts to roll-over only ≈ 0.2s after the beginning of the seeding. The most striking difference between N_2 seeding and $\langle n_e \rangle$-ramp appears to be the behavior of the integrated ion flux to the inner target, Γ_t^i, plotted in panel e) of figure 2. While in the $\langle n_e \rangle$-ramp, a continuous increase is seen, the N_2-seeding scenarios show a decrease of Γ_t^i, an indication than the inner strike point remains attached in the $\langle n_e \rangle$-ramp while it detaches in the N_2-seeding cases. Bolometric measurements show that in the high-density N_2-seeding case, the radiation at the X-Point is already close ($\sim 20\%$ lower) to the radiation along the leg before the seeding (panel d) of figure 2). As N_2 is injected, it quickly becomes more prominent that radiation along the leg. In the low-density N_2-seeding case and in the $\langle n_e \rangle$-ramp, three radiations regions are initially present near the X-Points and both strike-points. As density is increased or N_2 is seeded, the radiation region near the X-Point becomes more prominent and the radiation peak along the outer leg moves towards the X-Point. This is apparent from panel d) of figure 2, where the ratio of the radiated power along the leg to the radiated power close to the X-Point quickly drops. In all cases, the radiation peak along the outer leg starts to move just before the rollover of Γ_t^o (panel g). Observations of the Carbon-III emission with a Multi-Spectra-Imaging system (MSI) also reveal a similar behavior of the CIII-front in the $\langle n_e \rangle$-ramp [2]. Measurements with a divertor spectroscopy system show that recombination rates remain low, while the decrease of the ionization source in the divertor is likely responsible for the observed drop of Γ_t^o [3, 4].

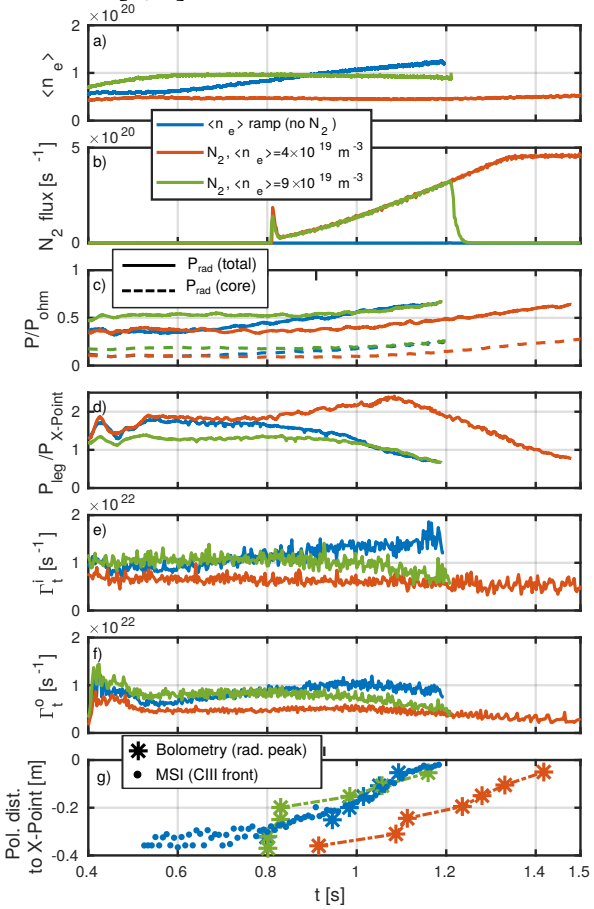

Figure 2: General evolution of $\langle n_e \rangle$-ramp and N_2-seeding L-Mode scenarios

Influence of geometry To check the influence of the plasma geometry on the N_2-seeding efficiency, f_x and target major radius R_t scans were performed. Both these parameters are supposed to be beneficial for the access to detachment at large values [1]. However, besides a slightly different Γ_t^o before the seeding starts, no significant difference has been observed on the dynamics of integrated or peak ion flux to the outer target.

Development of a pressure drop

In figure 3, the comparison of the target pressure p_{ds} (as measured by Langmuir probes) and of the upstream pressure p_{us} (measured either by a Thomson diagnostic or by a fast reciprocating probe) show in all three cases a reduction of p_{ds}, and the development of a drop between p_{us} and p_{ds}, which confirms the onset of detachment in these plasmas. Using a set of reciprocating probe plunges at different times throughout identical discharges, we reconstruct p_{us} as a function of time. The profile is then fitted by a decaying double-exponential. p_{ds} is fitted by an Eich's fit-like function. By integrating those fits, a global pressure drop can be estimated as

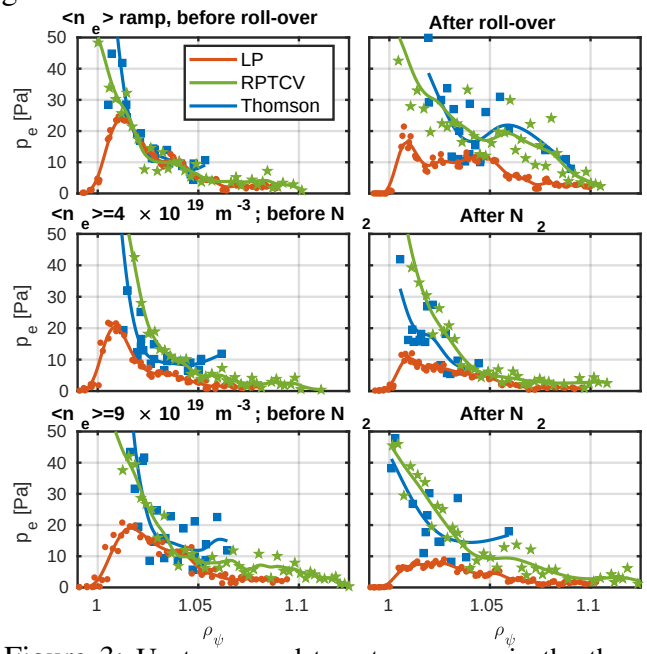

Figure 3: Upstream and target pressures in the three studied cases, for $f_x = 10$.

$$\Delta_p = \frac{\int p_{ds}^{fit} \mathrm{d}\rho}{\int p_{up}^{fit} \mathrm{d}\rho} \tag{1}$$

where the integrals are taken either from $\rho = 1$ to 1.1 or from the location of the peak of the target profile up to $\rho = 1.1$. In figure 4, we have plotted the evolution of Δ_p as a function of time in the case of a $\langle n_e \rangle$-ramp and in the high-density, N_2-seeding case. In both situations, we observe the decrease of Δ_p, an indication that momentum losses are occurring in the divertor. The extent of the pressure drop Δ_p appears to be smaller in the N_2-seeding experiments, although experimental uncertainties (both on the pressure measurements and profile alignment between upstream and targets) prevent a precise quantitative estimate. It should be noted that the $\approx 70\%$ drop found in the $\langle n_e \rangle$-ramp is consistent with previous results in TCV, where the Self-Ewald model (based on the assumption that the momentum losses are only due to charge-exchange, whose rate compared to ionization is estimated by spectroscopic measurements) predicted a similar level of pressure drop [4].

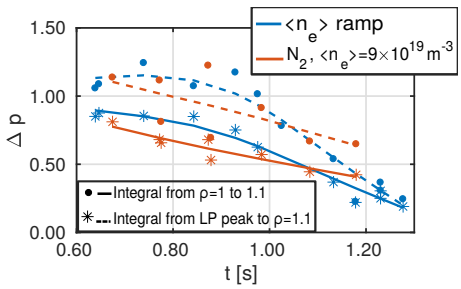

Figure 4: Evolution of the pressure drop Δ_p. The lines are cubic-spline fits.

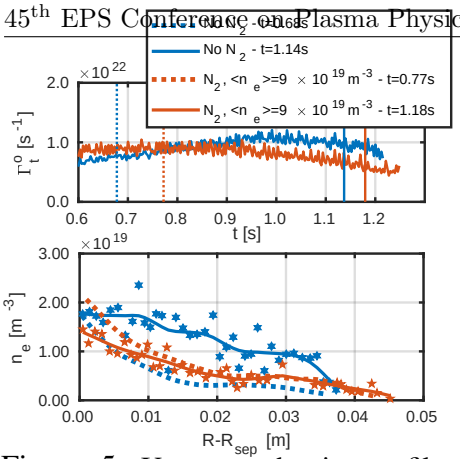

Figure 5: Upstream density profiles for $\langle n_e \rangle$-ramp and N_2-seeding, obtained by a reciprocating probe.

Evolution of upstream density profile The observation of the upstream density profiles ($f_x = 10$) further reveals the onset of a density shoulder in the $\langle n_e \rangle$-ramp case, as discussed previously in [2, 5]. In the N_2-seeding discharges however, no such behavior is observed, as shown in figure 5. It should be noted that the onset of a density shoulder in the $\langle n_e \rangle$-ramp case coincides with the roll-over of Γ_t^o, although a causality relation between the two cannot be inferred. However, by "raising" the upstream density of flux tubes at $\rho > 1$, the formation of a shoulder may contribute to the propagation of the detachment away from the separatrix. Furthermore, due to the broadening of the density profile, the shoulder could potentially modify the plasma-wall interaction at the outer-midplane, resulting for instance in a lower outer target ion flux after detachment or enhanced power losses due to additional carbon erosion at the main wall. However, a scan in the outer gap value has shown that this effect is not sensitive to the value of the outer gap.

Summary In this paper, we summarized the main observations of the L-Mode N_2 detachment experiments in TCV. At both low- and high- $\langle n_e \rangle$, a drop of the target ion flux is observed after the injection of N_2. The inner strikepoint detaches in N_2-seeded discharges, while it remains attached in $\langle n_e \rangle$-ramp. No clear effect of the geometry could be seen on the dynamics of detachment with N_2 seeding. The comparison of upstream and target profiles shows, both for N_2 seeding and density ramps, the presence of a pressure drop along SOL field lines, which proves the detached state of the divertor. In the high-density seeding case, a series of probe plunges in repeat discharges allowed to further quantify the evolution of the pressure drop, which appears to be lower than in the $\langle n_e \rangle$-ramp experiments, although precise quantification is difficult. No density shoulders are observed in N_2 seeding, unlike in the $\langle n_e \rangle$-ramp. Such behavior is consistent with observations on JET [6]. These experiments pave the way to the study of H-Mode, N_2-seeded detached scenarios at TCV that are now under investigation.

Acknowledgment This work was supported in part by the Swiss National Science Foundation. This work has been carried out within the framework of the EUROfusion Consortium and has received funding from the Euratom research and training programme 2014-2018 under grant agreement No 633053. The views and opinions expressed herein do not necessarily reflect those of the European Commission.

References

[1] C. Theiler *et al.*, Nucl. Fusion **57**, 072008 (2017)
[2] J. Harrison *et al.*, Nucl. Mat. Ener. **12**, 1071-1076 (2017)
[3] K. Verhaegh *et al.*, Nucl. Mat. Ener. **12**, 1112-1117 (2017)
[4] K. Verhaegh *et al.*, *in preparation*.
[5] N. Vianello *et al.*, Nucl. Fusion **57**, 116014 (2017)
[6] A. Wynn *et al.*, Nucl. Fusion **58**, 056001 (2018)